UNIVERSITY OF CALIFORNIA, SAN DIEGO

Development of Quantitative Real Time PCR to Assess Human Brain Microvascular Endothelial Cell Susceptibility to HIV-1 Infection

A thesis submitted in partial satisfaction of the requirements
for the degree Master of Science

in

Biology

by

Ying Sheng Chao

Committee in charge:

Professor Teresa Dianne Langford, Chair
Professor Michael David, Co-Chair
Professor Immo E. Scheffler

2008

The Thesis of Ying Sheng Chao is approved and it is acceptable in quality and form for publication or microfilm:

_____

_____

Co-Chair

_____

Chair

University of California, San Diego

2008

DEDICATION

To E.G.

TABLE OF CONTENTS

LIST OF FIGURES

LIST OF TABLES

ACKNOWLEDGEMENTS

First and foremost, I thank Dr. Dianne Langford for providing me this invaluable opportunity to participate in her research for the past three years. The experience has been the most intellectually challenging, nurturing, and has made me who I am today. I couldn't express enough gratitude for her support, understanding and guidance.

I thank Dr. Michael David and Dr. Immo Scheffler for their willingness to participate in my research committee despite their busy schedules. Their advices and suggestions have been tremendously constructive and enlightening. I couldn't have done it without them.

Last but most importantly, I am deeply indebted to my parents for their patience and unconditional giving.

ABSTRACT OF THE THESIS

Development of Quantitative Real Time PCR to Assess Human Brain Microvascular Endothelial Cell Susceptibility to HIV-1 Infection

by

Ying Sheng Chao

Master of Science in Biology

University of California, San Diego, 2008

Professor Teresa Diane Langford, Chair

Neuroimaging studies identified blood brain barrier disruption as a common feature in HIV associated dementia (HAD) and suggested that human brain microvascular endothelial cells (HBMECs) are involved in neuropathogenesis. Direct infection of HBMECs by HIV-1 has been reported by in vivo and in vitro studies, yet data interpretation has been compounded by technical limitations and productive infection has not been reproducible. Variability between these studies is very likely the result of

different HIV-1 strains employed and unidentified host factors affecting the eventual outcome.

The main goal of the present study is to address the possibility of intracellular restriction to HIV-1 replication in HBMECs. Toward this goal, a VSV-G pseudotyped HIV-1 NL4-3 virus was constructed which could mediate cytoplasmic delivery in the apparent absence of appropriate host cell receptors and a series of qRT-PCR assays were developed to monitor HIV-1 lifecyle progression in HBMECs. Overall, the qRT-PCR assays were demonstrated to be specific, sensitive, efficient, cover a dynamic linage range, and reproducible. Utilizing these qRT-PCR assays, it was shown that HBMECs exhibit comparable reverse transcription, provirus integration, yet a diminished early regulatory gene expression exemplified by *rev* transcription. Interestingly, late gene expression and whole genome replication, indicated by the detection of comparable number of *gag* transcripts, were not affected. However, it was shown that HBMECs might promote a modification, or degradation of HIV-1 p24 capsid protein.

Introduction

In addition to the hallmark immune system dysregulation and dysfunction, another major clinical feature of HIV-1 infection is penetration of the virus into the central nervous system (CNS). Neurological involvement is observed in 60% of HIV-1 patients (Fischer-Smith T, 2005) and HIV associated dementia (HAD) is documented in approximately 20% of HIV-1 positive individuals (Moses *et al*., 1996). Since the advent of highly active anti-retroviral treatment (HARRT), a milder form of HAD, minor cognitive motor disorder, has been documented and reported to be more prevalent, up to 30%, possibly due to the longer life spans and the slower progression to classically defined HAD of HIV positive patients on HARRT (Gonzalez-Scarano *et al*., 2005). Neuropathologically, HAD is characterized by infiltration of HIV-gp41 immunoreactive monocytes/macrophages and lymphocytes, widespread myelin loss, axonal injury, microgliosis and astrogliosis (Langford *et al*., 2002). Along with the observation of neural apoptotic cell death (Pettito *et al*.,1995), these findings suggest CNS inflammation and neurodegeneration as events instrumental for the development of HAD. Clinical features of HAD include slowing in motor function, cognitive ability impairment and behavioral changes, which are commonly described as Parkinsonian (Berger *et al*., 2000). Considering the debilitating nature of HAD and now the longer life span of HIV-1 patients, a better understanding of the mechanisms and factors leading to HAD is allow a more specifically targeted therapy.

Against the backdrop of gross neurodegeneration in the CNS, contrast-enhanced magnetic resonance imaging studies have identified BBB compromise as a common feature of HIV infection (Berger *et al*, 2000). In another study employing the same methodology, Avison et al. reported the correlation between the severity of HAD symptoms and the degree of blood brain barrier (BBB) disruption in the basal ganglia. This evidence not only corroborates on the subcortical nature of HAD, but also point to BBB impairment as a major factor contributing to neuropathogenesis. In healthy individuals, the CNS is largely insulated from the peripheral circulation by the BBB. Human brain microvascular endothelial cells (HBMECs) constitute the barrier by forming tight junctions between adjacent cells, restricting the diffusion of proteins, large molecules or even ions, and maintaining the stable ionic environment vital to the normal functioning of brain cells (Brightman *et al*., 1995). In HIV-1 infection, however, viral penetration into the CNS is clearly indicated by the presence of cell free viruses and viral antigens, possibly because HBMECs are being affected or exploited in some way resulting in the loss of BBB integrity. Indeed, numerous studies have identified viral and host inflammatory factors which can alter HBMEC cell biology and gene expression in favor of viral entry into the CNS (Andras *et al*., 2003, Chaudhuri *et al*., 2007).

Theoretically, one contribution to virus entry into the CNS is direct infection of HBMECs followed by the release of progeny virions into the CNS. Indeed, in vivo HIV-1 infection of HBMECs has been reported by studies employing immunohistochemistry of HIV RNA by in situ hybridization (ISH) (Wiley *et al*., 1986, Ward *et al*., 1987,) and RT-PCR-ISH (An *et al*., 1999). However, the status of HBMEC susceptibility to HIV-1 has remained largely unresolved due to difficulties in interpreting these data. Major criticisms include the lack of double labeling demonstrating the localization of HIV-1 antigens to true endothelial cells, the possibility of the mere attachment of antigens and the questionable biological significance of PCR-ISH (Bissel *et al*., 2004). Considering the inconclusive and contentious results obtained from in vivo results, in vitro experiments have been conducted employing quantitation of p24 in HBMEC supernatant and co-culture rescue. In one study, persistent infection of HBMECs by HIV-1 LAI was demonstrated by the detection of p24 antigen using immunostaining up to 4 weeks post-infection (Moses *et al*., 1993). In another study, it was reported that HBMECs are not productively infected but that HIV-1 can be rescued by co-culture with cells that are susceptible to infection (Poland *et al*., 1995). Like their in vivo study counterparts, the methodology of these in vitro studies have also been questioned on the ground of methodology. In the latter case, it is argued that the viruses rescued could be cell surface associated but not true progeny as the result of a productive infection (Bissel *et al*., 2004). Overall, the status of

HBMEC susceptibility to HIV-1 infection is unresolved and may be due in part to the lack of rigorous demonstration of HIV internalization by a homogenous population of HBMECs, the lack of quantitation in PCR studies, and the unidentified sources of variability between studies.

It is generally believed that HBMECs are not susceptible to HIV-1 infection in the traditional sense because they lack CD4, the primary receptor for HIV. However, various moieties on HBMECs, such as sialic acid, N-acetylglucosamine, lipid rafts and proteoglycans have been shown to mediate HIV-1 entry through the endocytic route (Banks 2001 *et al*., Liu *et al*., 2002, Argyris *et al*., 2003). Among these reports, some argued that most of these virions are trapped and inactivated by acidification of the late endosome/lysosome, while others have shown that some virions can be transcytosed to the CNS. In T lymphocytes, the endocytic route is not a dead end for HIV-1 infection as cytoplasmic delivery of the viral genome can still commence when CD4 receptors *in* the endosome mediate membrane fusion between the host cell and virion (Schaeffer *et al*., 2004). However, this may not be the case for HBMECs even if HIV-1 virions are endocytosed, since HBMECs do not express CD4 receptors. On the other hand, strains of HIV-1 actually *requiring* acidic activation of gp41 for cytoplasmic delivery via the endocytic route have been reported (Cheng-Mayer C *et al*., 1987, Clapham PR *et al*., 1996, Fackler 2000).

In summary, conclusions on HBMEC susceptibility to HIV-1 could be very much dependent on the HIV-1 strains and methodologies employed. It is also very likely that the outcome of HIV-1 interaction with HBMECs is modulated by not yet identified host and viral factors. In addition, HBMECs may permit viral cytoplasmic delivery, contrary to conventional wisdom, but harbor intracellular blocks to virus replication. The examination for and the elucidation of potential intracellular restriction mechanisms may be important ways through which novel therapeutic targets and treatments can be identified and developed. The first aim of the current study is to develop a series of qRT-PCR assays which are sensitive and specific to HIV-1 nucleic acid that is indicative of each stage of the viral lifecycle. The second aim is to construct a pseudotyped HIV-1 virus that can enter HBMECs independent of CD4, subsequently permitting the investigation of intracellular restriction employing the qRT-PCR assays in HBMECs.

Materials and Methods

Human Brain Microvascular Endothelial Cell Culture

Human brain microvascular endothelial cells (HBMECs) were purchased from Cell Systems Corporation (Kirkland, WA) and routinely cultured at 37ºC, 5% CO_2 with endothelial cell medium (ScienCell Research Laboratories, Carlsbad, CA) 10% heat inactivated fetal bovine serum, endothelial cell growth supplement and penicillin/streptomycin solution. HBMECs were passaged before 90% confluence was reached. For infection experiments, 1.6 × 10^5 cells per well were plated in 6-well plate, exposed to 0.2 MOI wild type or VSV-G pseudotyped HIV-1 NL4-3, then spinoculated at 3,000 rpm for 60 minutes at room temperature in a Sorvall RT7 tabletop centrifuge. For up to 96 hours after exposure, HBMECs were collected using 1mg/ml pronase. DNA, RNA and proteins were extracted at various time points.

U373 MAGI cell culture

U373 glioblastoma cells expressing CD4, CD4 plus CXCR4 and CD4 plus CCR5, cat#3595, 3596, 3597, respectively, were obtained from Dr. Michael Emerman through the AIDS Research & Reference Reagent Program. In this particular cell line denoted U373 MAGI (multinuclear activation of a galactosidase indicator), a single copy integrated β-

galactosidase gene under the control of HIV-1 LTR is expressed in the presence of transactivating protein Tat. Cells were maintained in DMEM supplemented with 10% heat inactivated fetal bovine serum in the presence of 0.2 mg/ml G418 and 0.1 mg/ml hygromycin B for CD4 U373, and additionally, 1.0 µg/ml puromycin for U373 CXCR4 and CCR5. Cells were passaged before 90% confluence is reached 1:4 twice per week. Cells used for tittering viral preparation were used for no more than 15 passages. For infection studies, 2.5 ×10^5 cells per well were plated in 6-well plate, exposed to 0.2 MOI wild type or VSV-G pseudotyped HIV-1 NL4-3, then spinoculated at 3,000 rpm for 60 minutes at room temperature in a Sorvall RT7 tabletop centrifuge. For up to 96 hours after exposure, U373 MAGI CXCR4 cells were collected using 1mg/ml pronase. DNA, RNA and proteins were extracted at various time points.

PBMC isolation

Human whole blood was purchased from Biological Specialties Corporation (Colmar, PA). Briefly, 15 ml of human whole blood was mixed with 15 ml of 1X PBS, underlaid with 12.5 ml Ficoll-Paque PLUS (GE healthcare, Piscataway, NJ), then subjected to centrifugation at 1000 rpm in a Sorval RT7 tabletop centrifuge for 45 minutes at room temperature. After centrifugation, PBMCs were collected in the gray interface layer between

serum and Ficoll-Paque. Cells were then removed and washed 3 times in 1X PBS, subsequently plated in RPMI 1640 medium supplemented with 15% heat inactivated FBS, 2 mM L-glutamine, 100 units/ml penicillin, 100 ug/ml streptomycin and stimulated with 3 ug/ml phytohemagglutinin and 2 ug/ml polybrene for 3 days before proceeding with virus expansion co-culture protocol.

HIV-1 primary isolates propagation

Primary HIV-1 isolates were propagated and expanded in PHA-stimulated PBMCs. The expansion and co-culture protocol was adapted from *Propagation of Primary HIV-1 isolates* DAIDS Virology Manual for HIV laboratories, publication NIH-97-3838. Briefly, 40 ×10^6 PBMCs were stimulated for 3 days with 3 ug/ml phytohemagglutinin then exposed to virus in co-culture medium composed of 15% heated-inactivated fetal bovine serum (FBS), 20 units/ml Il-2, 2 mM L-glutamine, 2 ug/ml L-glutamine, 100 units/ml penicillin, 100 ug/ml streptomycin and 2 ug/ml polybrene. Cells were co-cultured with virus stock and the culture was monitored daily for up to day 10 or terminated when p24 reached or exceeded 200 ng/ml. Subsequently, supernatant was clarified by centrifugation twice in a Sorvall RT7 tabletop centrifuge, 1400 rpm for 10 minutes then 2400 rpm for 10 minutes at room temperature. Residual cell debris was further removed by filtering the

supernatant through a 0.22 um membrane. To remove potential carried-over cellular or viral DNA, supernatant was subjected to 15 U/ml DNase for 60 minutes at room temperature. To further concentrate the virus, the supernatant was ultracentrifuged at 25,000 rpm for 2 hours in a Beckman Coulter SW28 rotor at room temperature. Virus pellets were resuspended in 1X PBS by vortexing at low speed for 1 hour at room temperature. Concentrated virus stocks were divided into 50 µl aliquots and stored at -80ºC. MAGI assay was subsequently performed to quantitate virus concentration and titer transduction units.

VSV-G pseudotyped NL4-3 HIV-1 production

293FT, a clonal derivative of the parental human embryonal kidney cells which stably expresses the large T-antigen for enhanced viral titer was purchased from Invitrogen Corp. (Carlsbad, CA) and propagated as instructed. Cells were routinely cultured in complete medium composed of DMEM (high glucose), 10% heat inactivated FBS, 0.1 mM MEM non-essential amino acids, 6 mM L-glutamine, 1 mM MEM sodium pyruvate, 1% pen-strep, and 500 µg/ml Geneticin (Invitrogen Corp., Carlsbad, CA). Cells were maintained in a 37ºC and 5% CO_2 incubator and passaged before reaching 90% confluence. The vector plasmids utilized included pNL43.Luc.R-E-, obtained from the NIH AIDS Research and Reference Reagent Program, Division of AIDS, NIAID, NIH

from Dr. Nathaniel Landau and pLP/VSV-G (Invitrogen, Carlsbad, CA). To produce VSV-G pseudotyped NL4-3 HIV-1, the following transfection and collection scheme was followed. One day before transfection, 3 ×10^6 293FT cells were plated onto 100 mm diameter tissue culture dishes and allowed to adhere overnight. The next day, at 60% confluence, 293FT cells were transfected with 10 µg pNL43.Luc.R-E- and 3 µg pLP/VSV-G using $CaCl_2$ solution of the following composition: 110 mM NaCl, 25 mM BES, 0.75 mM Na_2HPO_4 and 250 mM $CaCl_2$. Supernantant was collected and fresh medium was added at 24h, 48h, and 96h post-transfection. Supernatant was pooled and clarified by centrifugation at 1400 rpm for 10 minutes followed by a second centrifugation at 2400 rpm for 10 minutes at room temperature in a Sorvall RT7 tabletop centrifuge. Residual cell debris were further removed by filtering via a 0.22 µm filter. Viruses were concentrated by ultracentrifuation in a Beckman Coulter SW28 rotor at 25,000 rpm for 2 hours at room temperature. Virus pellets were resuspended in PBS by vortexing at low speed at room temperature for 1 hr. Concentrated virus stocks were divided into 50 µl aliquots and stored at -80ºC. The MAGI assay was subsequently performed to quantitate virus concentration and titer transduction units.

MAGI assay

6 × 10^4 U373 MAGI cells were plated in 12 mm 24-well plate one day before exposure to virus. The cells were approx. 40% confluent the next morning. The medium was aspirated and cells were rinsed once with 1X PBS before exposure to virus in 500 µl of fresh medium. The cells were centrifuged at 3000 rpm in a Sorvall RT7 tabletop centrifuge for 60 minutes at room temperature and incubated at 37ºC in 5% CO_2 humidified incubator. Forty-eight hours later, cells were fixed and stained for β-galactosidase activity using an in situ β-galactosidase staining kit (Stratagene, La Jolla, CA). The staining solution was left on for 5 hours then blue cells were counted under a light microscope, and the transduction units (IU) were expressed as the number of blue cells per µl virus stock.

Quantitative real-time PCR

Total RNA and DNA were purified using the RNeasy and DNeasy kits, respectively (Qiagen, Valencia, CA). cDNA was synthesized as described in the iScript cDNA synthesis kit manual (Qiagen, Germantown, MD). Briefly, 1 µg RNA was combined with 5X reaction buffer, 1 µl reverse transcriptase and water to a final volume of 10 µl, which was incubated at room temperature for 5 minutes, 42ºC for 30 minutes, then 85ºC for 5 minutes. The SYBR Green Supermix (Bio-rad, Hercules, CA) was used on an iQ5-iCycler instrument (Bio-Rad). RT-PCR reactions were carried out in a total volume of 20 µl containing

100 ng DNA or cDNA with the appropriate thermocycling steps, then dissociation curve data collection was conducted with 40 cycles of 1ºC/10 s increases in temperature starting at 60ºC. Each sample was assayed in triplicate and no-template-controls were included. Human ribosomal 16s rRNA gene was assayed as a reference gene to control for unintended differences in the amount of cDNA or DNA used. Absolute copy number was extrapolated using a best-fitted line of the Ct values of serially diluted cDNA samples of known concentrations.

HIV-1 *gag* detection

Primers specific for HIV-1 *gag* were synthesized by ValueGene (San Diego, CA). Using these primers, HIV-1 RNA whole genome and HIV-1 *gag* transcripts are indiscriminately detected. Forward and reverse primers were used at 300 nmol. The PCR reaction was performed with the following parameters: initial denaturation 95ºC for 3 min, 40 cycles of denaturation at 95ºC for 10 s, annealing at 62.3ºC for 30 s, then dissociation curve data collection with 40 cycles of 1ºC/10 s increases starting at 60ºC. Primer sequences were obtained from Vandegraaff *et al.* 2001: Gag-PI(+)5'-GAG GAA GCT GCA GAA TGG G-3'; Gag-III(-) 5'-TGT GAA GCT TGC TCG GCT C-3'.

HIV-1 late reverse transcription product detection

To assess HIV-1 reverse transcription late product which has completed both strand transfers, primers specific for the region spanning the 3' of LTR and the 5' of *gag* gene were used (Butler *et al*., 2001). Forward and reverse primers were used at 300 nmol. The PCR reaction was performed with the following parameters: initial denaturation at 95ºC for 3 min, 40 cycles of denaturation at 95ºC for 10 s, annealing at 62.3ºC for 30 s, then dissociation curve data collection with 40 cycles of 1ºC/10 s increases starting at 60ºC. Primer sequences were obtained from Bushman et al 2000 and synthesized by ValueGene (San Diego, CA): MH531 forward 5'-TGT GTG CCC GTC TGT TGT GT-3'; MH532 reverse 5'-GAG TCC TGC GTC GAG AGA-3'.

Multiply spliced HIV-1 *rev* detection

To assess HIV-1 early gene expression, primers specific for HIV-1 *rev* mRNA were designed using Vector NTI (Invitrogen, Carlsbad, CA). Using these primers, only transcripts that span the *rev* exon1 and exon2 are amplified, thus ensuring the specific detection of multiply spliced rev mRNA. Forward and reverse primers were synthesized by ValueGene (San Diego, CA) and used at 300 nmol. The PCR reaction was performed with the

following parameters: initial denaturation 95ºC for 3 min, 40 cycles of denaturation at 95ºC for 10 s, annealing at 60ºC for 30 s and extension at 72ºC for 10 s, then dissociation curve data collection with 40 cycles of 1ºC/10 s increases starting at 60ºC. NCBI entry AF_003887 nucleotide sequence of the HIV-1 NL4-3 genome was used for primer design and selection targeting *tat/rev* using Invitrogen Vector NTI (Invitrogen, Carlsbad, CA). Primer sequences are as followed: HIV1/rev_400 forward 5'-AGG AAG AAG CGG AGA CAG-3'; HIV1/rev_401 reverse 5'-CCA CAA TCC TCG TTA CAG T-3'.

Western blotting

HBMECs and U373 MAGI CXCR4 cell lysates were collected using NE-PER Nuclear and Cytoplasmic Extraction Reagents (Pierce Biotechnology, Rockford, IL) and stored at -80ºC before use. Protein concentration was quantified by BCA assay (Pierce Biotechnology) and equal amount of proteins were used for all samples. Primary antibodies specific for Gag HIV-1 SF2 p24 antiserum NIH Cat#4250 produced by BioMolecular Technologies was obtained through the AIDS Research and Reference Reagent Program, Division of AIDS, NIAID, NIH. Western blotting was performed using SDS PAGE system (Invitrogen, Carlsbad, CA) and visualized by ECL reagents (PerkinElmer Life Sciences, Boston, MA). The blot image was captured by

VersaDoc (Bio-Rad, Hercules, CA) and quantified by Quantity One software (Bio-Rad).

Reagents

A nucleoside analogue which inhibits HIV-1 reverse transcription, zidovudine (AZT), was obtained through the AIDS Research and Reference Reagent Program, Division of AIDS, NIAID, NIH. AZT was reconstituted in DMSO and used at a working concentration of 25 μM. An azido-containing diketo acid derivative 118-D-24, hereafter DKA, which inhibits HIV-1 integrase, was obtained through the NIH AIDS Research and Reference Reagent Program, Division of AIDS, NIAID, NIH. DKA was reconstituted in DMSO nad used at a working concentration of 25 μM.

Chapter 1

Methodologies implemented to ensure proper control and independent evaluation of the PCR assays

Previous in vivo studies have demonstrated the presence of HIV antigens in HBMECs by immunocytochemistry and ISH but interpretation of the studies' data was confounded by the possibility that these antigens are simply adhering to the endothelial cell surface from the circulation rather than being internalized. In addition, technical difficulties have prevented double-labeling of viral antigens and cell-type specific markers, resulting in the identification of infected cell types relying solely on morphological appearance in possibly severely compromised preserved tissues, adding to the ambiguity in data interpretation (Bissel *et al*., 2004). Because of the aforementioned reasons, in vitro infection study is advantageous since it is more amenable to control measures and some of the shortcomings confounding in vivo data interpretation can be addressed. In this study aiming to investigate possible intracellular restriction on HIV-1 infection by HBMECs, a series of positive control measures were devised to allow a proper evaluation of the methodology being developed and data interpretation.

RESULTS:

A. Removal of cell surface associated virus with pronase

To ensure that only true infection or internalization events are detected by the PCR assays, pronase was used to remove cell surface associated

viruses. To demonstrate the effectiveness of pronase treatment, HBMECs were exposed to HIV at two temperatures, 37ºC and 4ºC in separate experiments, since viral internalization is permitted at 37ºC but inhibited at 4ºC (Argyris et al., 2003). Pronase or mock treatment in minimal medium was applied before cell lysis. Total RNA was purified and subjected to PCR detection of HIV RNA *gag*. Figure 1-1 shows that while pronase-treated cells exposed at 37ºC still retained a strong signal of HIV RNA *gag*, those exposed at 4ºC showed an undetectable level. In contrary, in mock treatment experiments, cells exhibited comparable *gag* level at both temperatures.

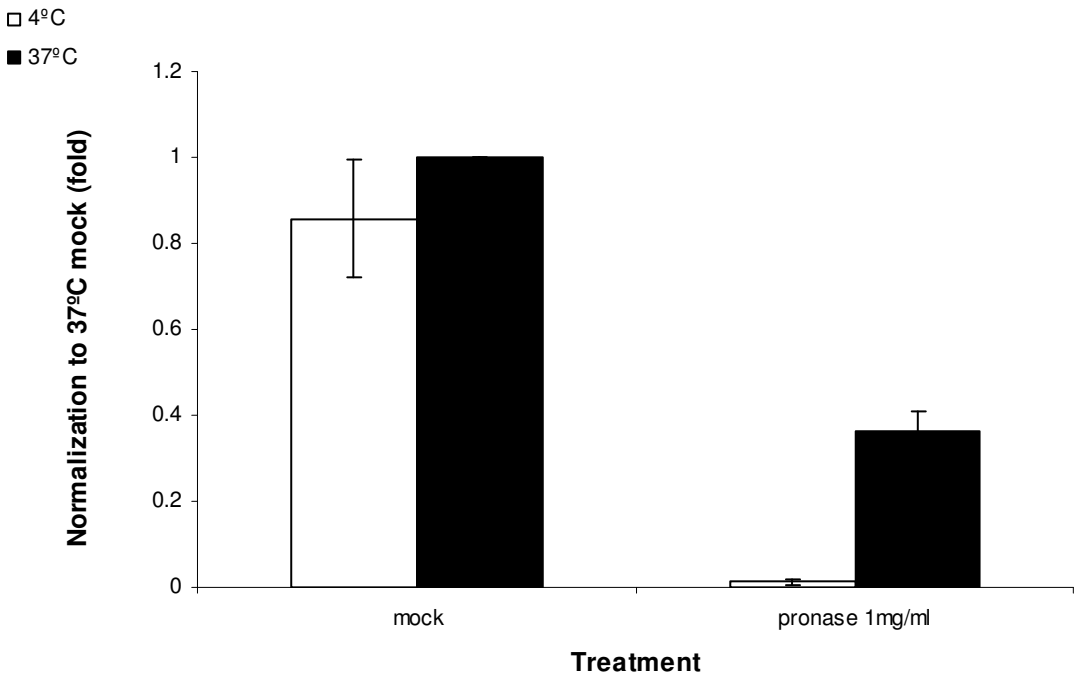

Figure 1-1. Pronase is effective at removing cell surface associated but not internalized virions. HBMECs exposed to 0.2 MOI wild type HIV-1 NL4-3 were collected by media aspiration followed by immediate exposure to pronase for 1 minute at room temperature. RNA was isolated, converted to cDNA, and subjected to qRT-PCR assay for *gag* quantitation. Error bars represent standard error.

B. Enhancement of infection by spinoculation

One potential problem with studies of HIV-1 infection of adherent cells in vitro is the limited infectivity displayed by wild type virus. Using a small volume for virus exposure that is usually employed with cells in suspension is not possible since a low volume of medium could evaporate relatively easier on a flat surface in the incubator in a short period of time. In order to examine the theoretical possibility and the course of infection in HBMECs, spinoculation was employed to ensure sufficient virus:cell contact (O'Doherty *et al*., 2000). In one experiment, to demonstrate the effectiveness of spinoculation at enhancing virus:cell contact, a comparison of the level of HIV RNA *gag* in HBMECs after different methods of virus exposure was conducted. Figure 1-2 shows that there is an approximately 20 fold enhancement of the amount of RNA *gag* in cells exposed then spinoculated for 1 hour at 3000 rpm over cells which were simply incubated with virus for 2 hours.

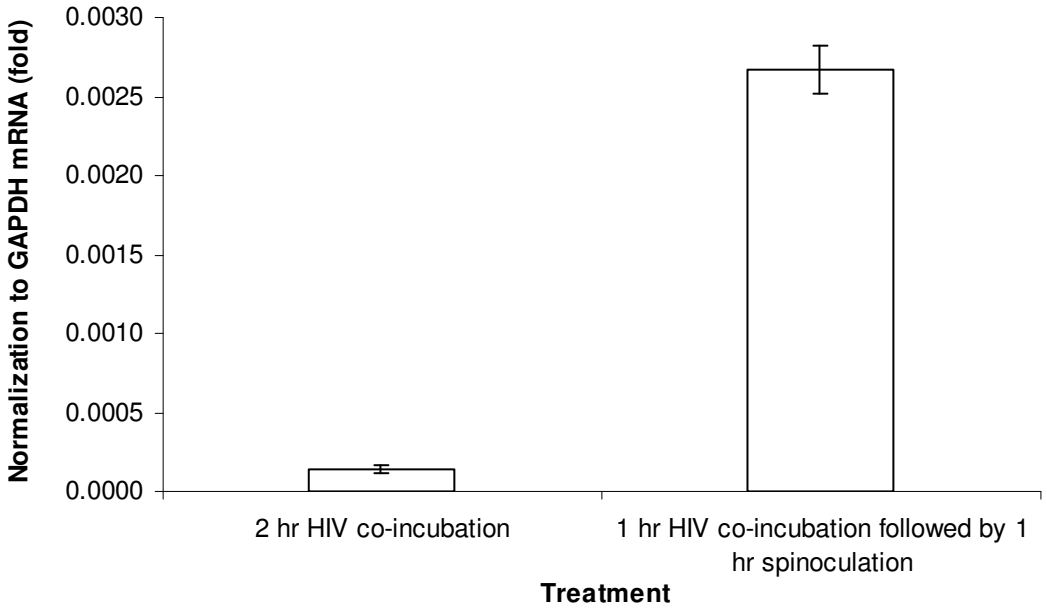

Figure 1-2. Spinoculation is effective at enhancing cell:virus contact and association. HBMECs were exposed to 0.2 MOI wild type HIV-1 NL4-3 then subjected to two methods of HIV-1 co-incubation as indicated by the figure. HBMCEs were collected using pronase, RNA was isolated, converted to cDNA and subjected to qRT-PCR assay for *gag* quantitation. Error bars represent standard error.

C. Efficient infection by VSV-G pseudotyped HIV-1 NL4-3 and visualization in U373 MAGI CXCR4 cells

In order to optimize the PCR assays, a system that would enable an abundant amount of viral nucleic acid to be detected and an independent mean to access the infection must be devised. In the case of HBMECs, which have been shown to undergo abortive or non-productive HIV infection, a means has to be developed to efficiently deliver the viral genome so that the course of infection can be assessed and the possibility of intracellular restriction investigated. These two goals were achieved utilizing VSV-G pseudotyped HIV-1 NL-43 and U373 MAGI cells. VSV-G envelope confers HIV-1 the ability to infect a range of host cells efficiently regardless of receptor or co-receptor usage, ensuring a course of infection including cytoplasmic delivery, reverse transcription, integration, early and late gene expression and subsequent replication. In addition, during the development of the PCR assays, efficient transduction ensures that an abundance of nucleic acids can be detected. Conveniently, the infection of U373 MAGI cells by HIV-1 can easily be visualized and quantified by β-galactosidase staining as shown in Figure 1-3, and can serve as an independent measure for the viability of the virus preparation and successful infection.

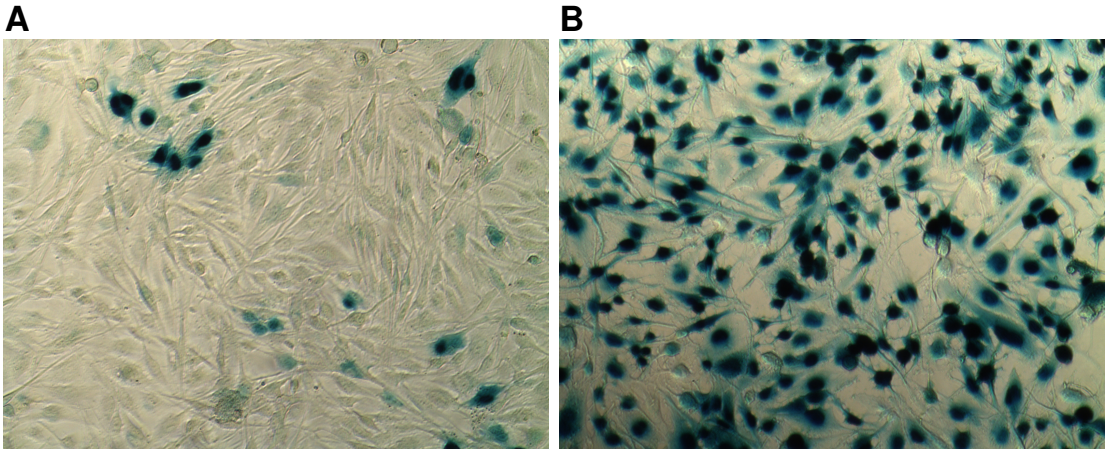

Figure 1-3. VSVG-pseudotyped HIV-1 NL4-3 exhibited enhanced infection of U373 MAGI CXCR4 cells. U373 MAGI CXCR4 cells were exposed to 0.2 MOI of either wild type HIV-1 NL4-3 (A) or VSV-G pseudotyped HIV-1 NL4-3 (B), spinoculated for 3000 rpm for 1 hour at room temperature, then incubated for 48 hours before staining for β-galactosidase activity.

Chapter 2

Development and optimization of qRT-PCR assays specific for different stages of the HIV-1 lifecycle

Numerous studies have reported and utilized the detection of viral nucleic acids as indicators of the extent of infection in various cell types (Schwartz *et al*., 1990, Mariani *et al*., 2000, Canki *et al*., 2001), yet this is the first time a series of assays are developed for the purpose of studying the entire HIV-1 life cycle in HBMECs with which the susceptibility to the virus is contended. A systematic study examining each step of the HIV lifecycle can not only provide a comprehensive overview of viral kinetic, but can also reveal the roadblock to infection in restrictive cell types. This information is valuable for identifying molecules or molecular mechanism which can be further studied and characterized for future therapeutic intervention.

Essential to the eventual productive infection of a host cell, HIV-1 nucleic acids progress through several conversions and modifications exploiting the host cell replication, transcription and RNA splicing machineries. This series of PCR assays was designed based on the premise that the presence of each type of viral nucleic acid is indicative of a particular step in the HIV-1 lifecycle. The detection and quantitation of each of these nucleic acids by qRT-PCR is a measure of how efficiently and to what extent has the HIV-1 lifecycle progressed. Once internalized by the host cell, viral RNA is exposed to the host cell cytoplasm upon disassembly of the nucleocapsid. At this stage, detection and quantitation of HIV-1 RNA is a measure of the degree of virus internalization. As the core is unpacked, viral RNA can be converted into cDNA by reverse transcriptase using the host's dNTP. At this stage,

detection and quantitation of viral cDNA is an indication of successful reverse transcription events. After viral cDNA is synthesized, it is associated with the viral integrase and several cellular host factors to form the pre-integration complex, which shuttles the HIV-1 cDNA into the host nucleus. Upon entry, HIV-1 integrase catalyzes the integration of viral cDNA into the host genome, a step that is essential to the transcription of HIV-1 genes and whole genome. At this stage, detection and quantitation of integrated provirus is a measure of integration efficiency. As transcription events are facilitated by the HIV-1 Tat protein, early transcripts of the regulatory *tat* and *rev* genes are subjected to the host RNA splicing machinery and are characteristically of the 4 kb sizes. Subsequently, as the amount of Rev proteins accumulate, full length or singly spliced viral RNAs of approximately 9 kb can be shuttled out of the nucleus, bypassing host mRNA splicing, facilitated by Rev. Once in the cytoplasm, structural proteins can be translated from these long transcripts and full length HIV-1 RNA genome can be packaged.

To accurately assess the extent of each step of the HIV-1 lifecycle progression in HBMECs, a quantitative and accurate measure of each viral nucleic acid type is crucial. To this end, individual qRT-PCR assay was optimized by adjusting the thermocycling parameters. The sensitivity, efficiency and linearity of the assays were assessed by constructing a standard curve using Ct values obtained from serial dilutions of a positive control template containing the region to be amplified. The intra- and inter-run

reproducibility of the assays was also assessed. Finally, the thermocycling parameters which yielded the highest sensitivity, efficiency and linearity were used for any subsequent experiments.

RESULTS:

A. Detection of RNA *gag* transcript and RNA whole genome

To quantitate HIV-1 RNA, forward primer Gag-PI(+) 5'-GAG GAA GCT GCA GAA TGG G-3' and reverse primer Gag-III(-) 5'-TGT GAA GCT TGC TCG GCT C-3' (Vandegraaff *et al.*, 2001) targeting HIV *gag* were used (Figure 2-1A). This primer set does not discriminate between whole genome RNA and *gag* transcripts. The quantitation is a general indication of the extent of HIV-1 internalization and subsequent replication. Figures 2-1B and 2-1C show that this assay covers a linear range of 1×10^6- 1×10^2 copies of *gag* with efficiency close to 100%. To assess the inter-run reproducibility of this assay, serial dilutions ranging from 1×10^6- 1×10^2 copies of a positive control template were performed 3 times over a course of 3 weeks. To assess the intra-run reproducibility of this assay, serial dilutions were performed in triplicate. The inter- and intra-run standard deviations and CV% are summarized in Table 1.

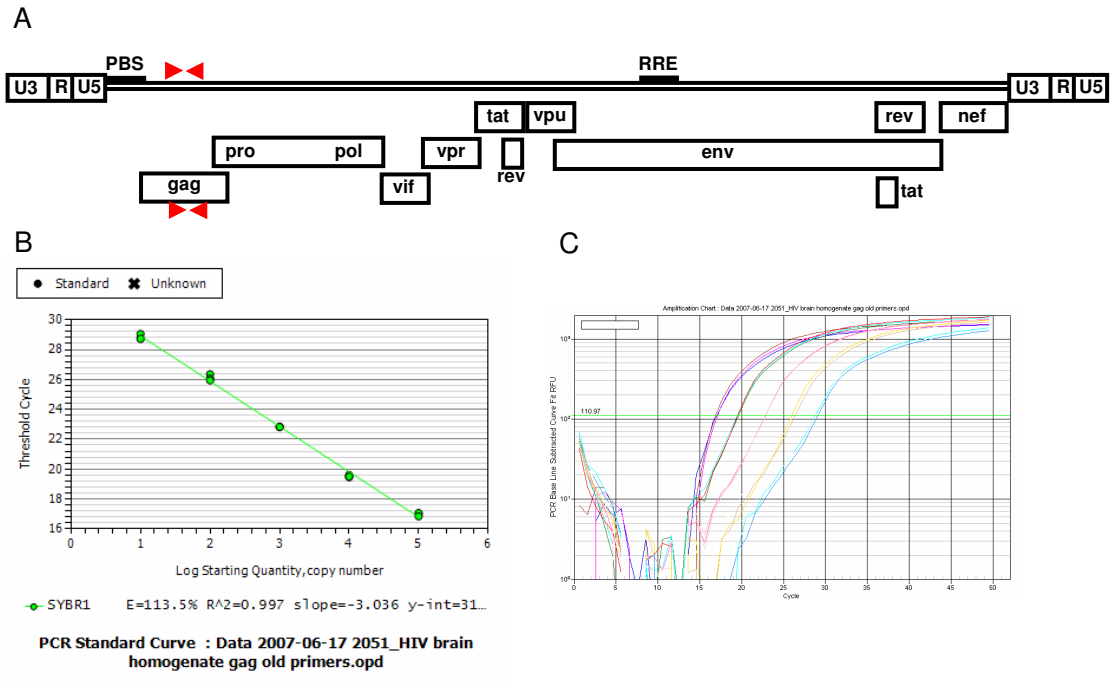

Figure 2-1. HIV-1 *gag* qRT-PCR assay exhibits a 5-log linear range and efficiency close to 100%. (A) Schematic representation of the HIV-1 genome and Gag-PI(+) and Gag-III(-) amplicon. (B) Linear curve correlating *gag* copy numbers to threshold cycle (Ct) values. (C) Amplification plot showing Ct values of *gag* 1 $\times 10^6$- 1 $\times 10^2$ copies.

TABLE 1. Intra- and inter-run reproducibility of *gag* qRT-PCR assay

	10^6	10^5	10^4	10^3	10^2
Intra-run					
Ct range	17.61-17.74	20.65-20.80	23.81-24.11	26.57-27.50	30.21-30.68
Ct mean	17.68	20.73	23.97	27.07	31.41
Ct Std Dev	0.06	0.08	0.15	0.47	0.24
Ct CV%	2.07	2.5	4.97	15.7	8.09
Inter-run					
Ct range	16.99-17.06	19.46-19.61	22.81-22.85	25.94-26.35	28.71-29.05
Ct mean	16.96	19.52	22.83	26.12	28.84
Ct Std Dev	0.12	0.08	0.02	0.21	0.19
Ct CV%	3.93	2.65	0.77	7.07	6.17

B. Detection of reverse transcribed cDNA

To quantitate HIV reverse transcription (RT) events, forward primer MH 531 5'-TGT GTG CCC GTC TGT TGT GT-3' and reverse primer MH532 5'-GAG TCC TGC GTC GAG AGA-3' (Butler *et al*., 2001) bridging HIV 5'LTR and 5' of gag gene were used (Figure 2-2A). This primer set detects HIV cDNA that has completed the second template switch, thus including both pre-integration HIV-1 cDNA and integrated provirus. Figures 2-2B and 2-2C show that this assay covers a linear range of 1×10^6- 1×10^1 copies with efficiency close to 100%. To assess the inter-run reproducibility of this assay, serial dilutions ranging from 1×10^6- 1×10^1 copies of a positive control template were performed three times over a course of three weeks. To assess the intra-run reproducibility of this assay, serial dilutions were performed in triplicate. The inter- and intra-run standard deviations and CV% are summarized in Table 2. To demonstrate the specificity of this RT assay, U373 MAGI cells expressing CD4 and CXCR4 receptors were exposed to wild type HIV-1 NL4-3 viruses plus DMSO or 25 μM AZT. Figure 2-3 shows that in the presence of AZT, the PCR assay quantitation of RT event was diminished by approximately 94 folds.

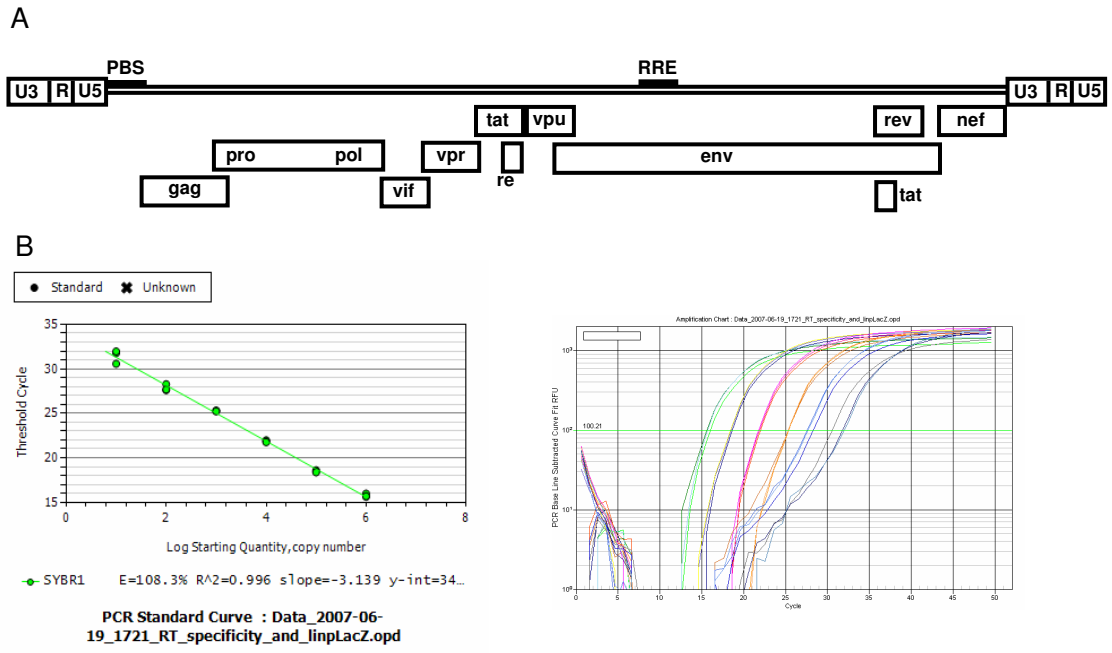

Figure 2-2. HIV-1 reverse transcription product qRT-PCR assay exhibits a 6-log linear range and efficiency close to 100%. (A) Schematic representation of the HIV-1 genome and MH531 and MH532 amplicon. (B) Linear curve correlating RT copy numbers to threshold cycle (Ct) values. (C) Amplification plot showing Ct values of reverse transcribed product 1 $\times 10^6$- 1 $\times 10^1$ copies.

TABLE 2. Intra- and inter-run reproducibility of reverse transcription product qRT-PCR assay

	10^6	10^5	10^4	10^3	10^2	10^1
Intra-run						
Ct range	14.48-14.6	17.94-18.35	21.3-21.72	26.02-26.05	29.72-31.05	31.59-32.36
Ct mean	14.65	18.14	21.57	26.17	29.93	32.01
Ct Std Dev	0.196	0.208	0.235	0.227	0.183	0.392
Ct CV%	6.53	6.93	7.83	7.57	6.10	13.07
Inter-run						
Ct range	15.63-15.98	18.37-18.61	21.76-21.97	25.23-25.31	27.61-28.28	30.57-31.95
Ct mean	15.76	18.48	21.86	25.27	27.86	31.43
Ct Std Dev	0.191	0.123	0.106	0.04	0.365	0.753
Ct CV%	6.37	4.10	3.53	1.33	12.17	25.10

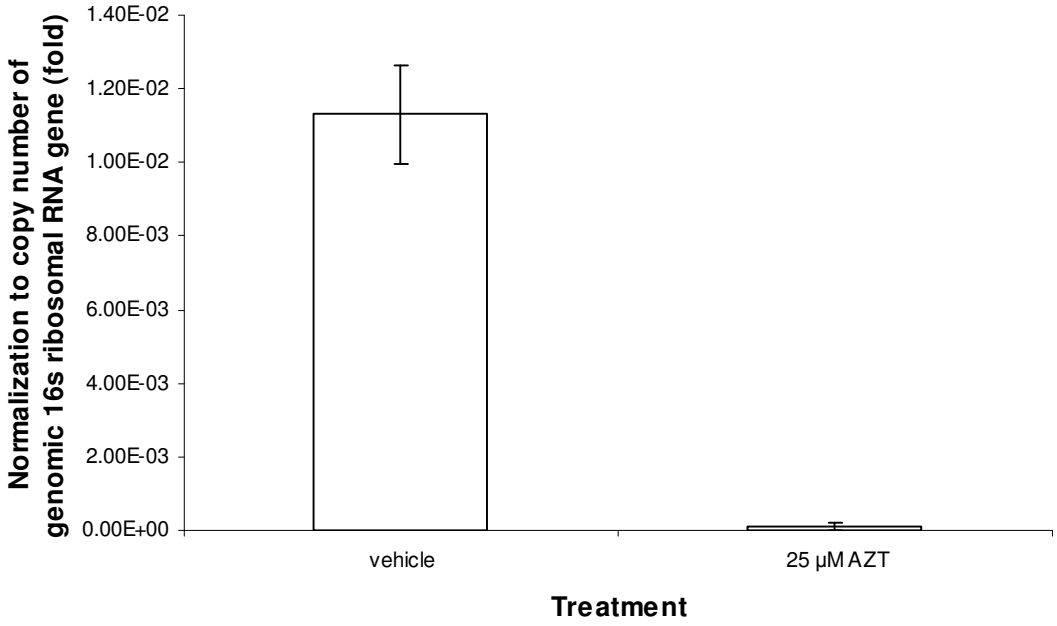

Figure 2-3. HIV-1 reverse transcription product qRT-PCR assay is specific for HIV-1 cDNA. U373 MAGI cells expressing CD4 and CXCR4 receptors were exposed to 0.2 MOI wild type HIV-1 NL4-3 in the presence of DMSO (vehicle) or 25 µM AZT. The quantity of HIV-1 RT cDNA in the AZT treated sample was significantly diminished compared to that in the DMSO treated sample. Error bars represent standard error.

C. Detection of multiply spliced *rev* transcripts

To quantitate multiply spliced HIV *rev* mRNA transcripts, forward primer rev_400 5'-AGG AAG AAG CGG AGA CAG-3' and reverse primer rev_401 5'-CCA CAA TCC TCG TTA CAG T-3' which span the tat and rev exons were used (Figure 2-4A). Detection of short ~4 kb transcripts by this primer set indicates early regulatory gene expression, which is essential for and precedes late structural gene expression. Since the forward and reverse primers span the two exons that make up the *rev* transcript, detection is only possible following transcription and RNA splicing. Figure 2-4B shows that this assay covers a linear range of 1×10^6- 1×10^2 copies with efficiency close to 100%. To assess the inter-run reproducibility of this assay, serial dilutions ranging from 1×10^6- 1×10^2 copies of a positive control template were performed three times over a course of three weeks. To assess the intra-run reproducibility of this assay, serial dilutions were performed in triplicate. The inter- and intra-run standard deviations and CV% are summarized in Table 3.

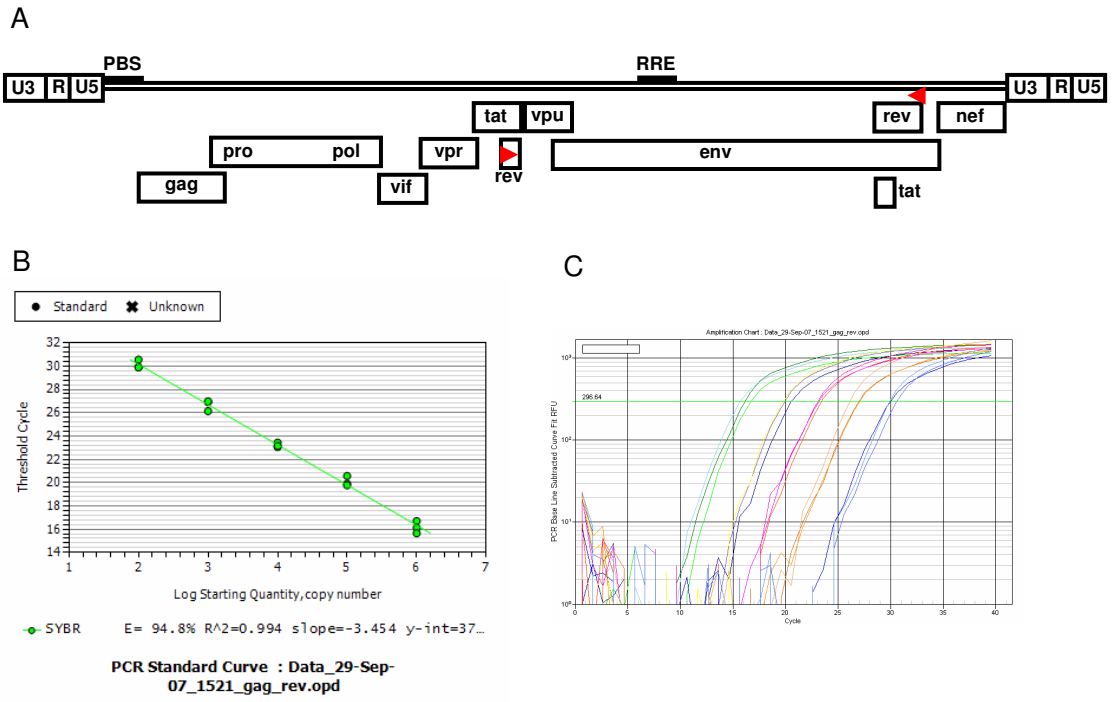

Figure 2-4. HIV-1 *rev* qRT-PCR assay exhibits a 5-log linear range and efficiency close to 100%. (A) Schematic representation of the HIV-1 genome and rev_400 and rev_401 amplicon. (B) Linear curve correlating RT copy numbers to threshold cycle (Ct) values. (C) Amplification plot showing Ct values of *rev* 1 $\times 10^6$- 1 $\times 10^2$ copies.

TABLE 3. Intra- and inter-run reproducibility of *rev* qRT-PCR assay

	10^6	10^5	10^4	10^3	10^2
Intra-run					
Ct range	16.96-17.48	20.93-21.2	24.63-24.63	26.52-29.05	31.15-31.86
Ct mean	17.15	21.09	24.68	28.04	31.53
Ct Std Dev	0.286	0.14	0.113	1.34	0.36
Ct CV%	9.53	4.67	3.77	44.67	12.00
Inter-run					
Ct range	15.65-16.7	19.77-20.57	23.05-23.43	26.14-26.98	29.89-30.57
Ct mean	16.16	20.08	23.21	26.68	30.13
Ct Std Dev	0.53	0.43	0.20	0.47	0.38
Ct CV%	17.50	14.30	6.67	15.57	12.67

Chapter 3

The examination for possible intracellular restriction of HIV-1 replication in HBMECs

Previous reports have demonstrated the lack of HIV-1 productive infection of HBMECs (Poland *et al*., 1995, Liu *et al*., 2002). Yet numerous studies, employing electron microscopy, have shown that HIV-1 virions are internalized in HBMECs. However, the outcome of this internalization is unclear. Most of the virions visualized by electron microscopy were localized to endosomes or lysosomes, leading to the predominant view that endocytosed virions are degraded in acidified compartments. In vitro, CD4 independent entry and post-endocytosis membrane fusion have been demonstrated with certain strains of HIV-1 (Cheng-Mayer C *et al*., 1987, Clapham PR *et al*., 1996, Fackler 2000). These findings raise the possibility that given the right combination of viral and host factors, HIV-1 can directly infect HBMECs, transcytose through the BBB and subsequently invade the CNS. However, despite the aforementioned evidence in favor of the susceptibility of HBMECs to HIV-1 infection, productive infection has been shown in only one report (Moses *et al*., 1993), raising the possibility that in addition to the receptor requirement, there are additional blocks to HIV-1 lifecycle progression in HBMECs. In order to investigate the possibility of intracellular restriction in HBMECs, a single round replication experiment was performed using an env-defective NL4-3 genome, NL4-3 env- hereafter, packaged with VSV-G envelope, thus bypassing the CD4 receptor requirement. Through this pathway, the HIV-1 genome is shuttled directly into the cytoplasm after VSV-G envelop-mediated endocytosis and acidic pH

induced cell membrane fusion. For comparison and as a positive control, U373 MAGI CXCR4, a glioblastoma cell line which is routinely used for titering HIV-1 virus preparations, was exposed to VSV-G pseudotyped HIV-1 NL4-3 in parallel experiments.

RESULTS:

A. HBMECs permit VSV-G envelope mediated internalization and replication of HIV-1 whole genome and *gag* transcripts

To assess total virion internalization and subsequent genome replication, HIV-1 *gag* specific reverse transcription qRT-PCR was performed on total RNA isolated from HBMECs and U373 MAGI CXCR4 cells exposed to 0.2 MOI VSV-G pseudotyped HIV-1 NL4-3 Env-. The detection of *gag* at the early time points up to 7 hr indicates the successful internalization of virions and whole genome. Amplification of the HIV-1 whole genome and presumably the subsequent splicing of the *gag* transcript occur at 12 h, followed by a peak of replication at 24 h for HBMECs, and 48 h for U373 MAGI CXCR4 cells (Figure 3-1).

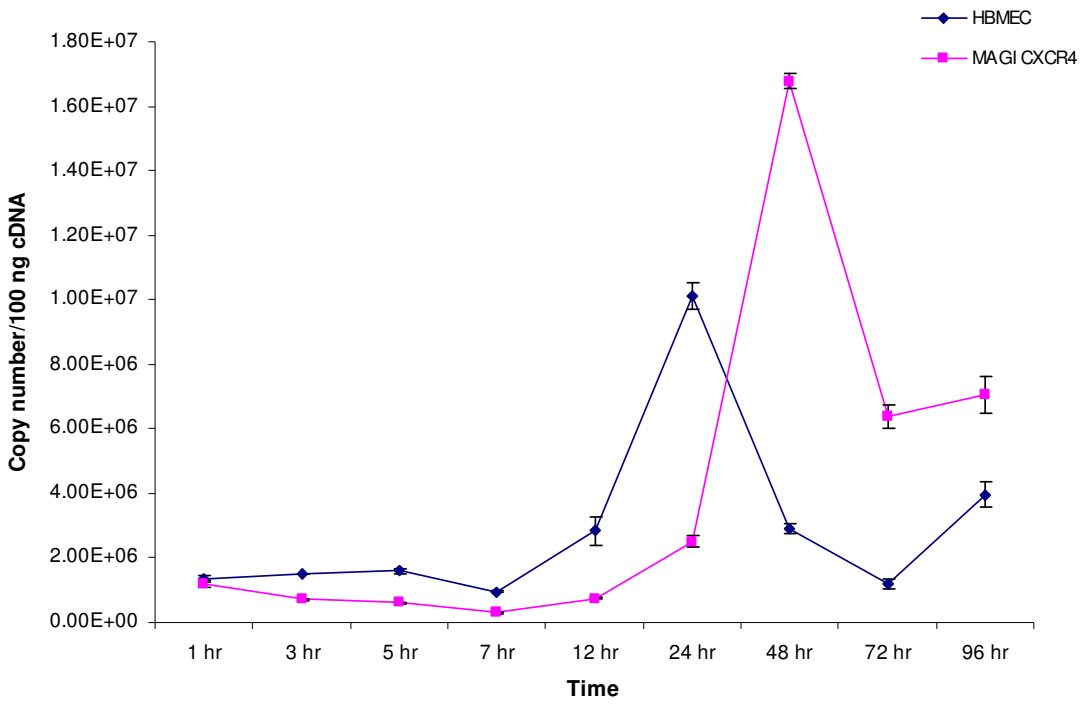

Figure 3-1. HBMECs are permissive to HIV-1 whole genome replication. HBMECs and U373 MAGI CXCR4 cells were spinoculated with 0.2 MOI of VSV-G pseudotyped HIV-1 NL4-3 in parallel. Total RNA was isolated at various times post-exposure and subjected to reverse transcription qRT-PCR detection and quantitation of *gag*. Figure 3-1 is representative of two qRT-PCR runs of the same experiment. Error bars represent standard error.

B. HBMECs permit HIV-1 reverse transcription

Since the HIV-1 whole genome was internalized and readily replicated, it appears that HBMECs are permissive of HIV-1 reverse transcription. Indeed, this was demonstrated by the detection and quantitation of HIV-1 reverse transcription product that had progressed through the two template switches required for HIV-1 cDNA synthesis (Butler *et al*., 2001). For both HBMECs and U373 MAGI CXCR4 cells, the synthesis of HIV-1 cDNA (Figure 3-2) preceded the amplification of whole genome and *gag* transcripts (Figure 3-1).

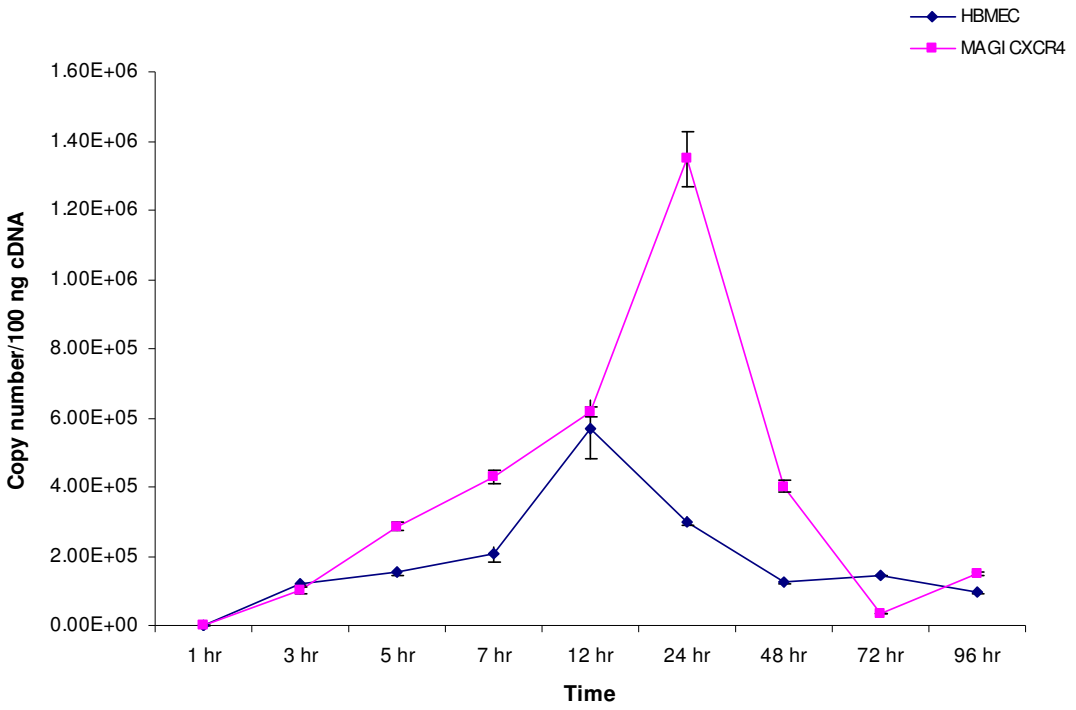

Figure 3-2. HBMECs are permissive of HIV-1 reverse transcription. HBMECs and U373 MAGI CXCR4 cells were spinoculated with 0.2 MOI of VSV-G pseudotyped HIV-1 NL4-3 Env- in parallel experiments. Total DNA was isolated at various times post-exposure and subjected to qRT-PCR detection and quantitation of HIV-1 cDNA. Figure 3-2 is representative of two qRT-PCR runs of the same experiment. Error bars represent standard error.

C. Integration is required for HIV-1 NL4-3 replication in HBMECs

An attempt was made to develop an assay specific for integrated HIV-1 provirus, however it was not successful, possibly due to one or more suboptimal parameters in the two step nested PCR. There have been reports showing that transcription is possible from unintegrated HIV-1 circular DNAs (Kelly *et al*., 2008). To demonstrate that the VSV-G pseudotyped HIV-1 NL4-3 env- undergoes integration as part of the natural infection and to validate this approach to investigate possible intracellular restriction, the effect of DKA, an integrase specific inhibitor, on HIV-1 RNA amplification was studied by employing qRT-PCR specific for the *gag* gene. As shown in Figure 3-3, HIV-1 total RNA propagation was significantly diminished by the addition of 25 μM DKA in both HBMECs and U373 MAGI CXCR4 cells.

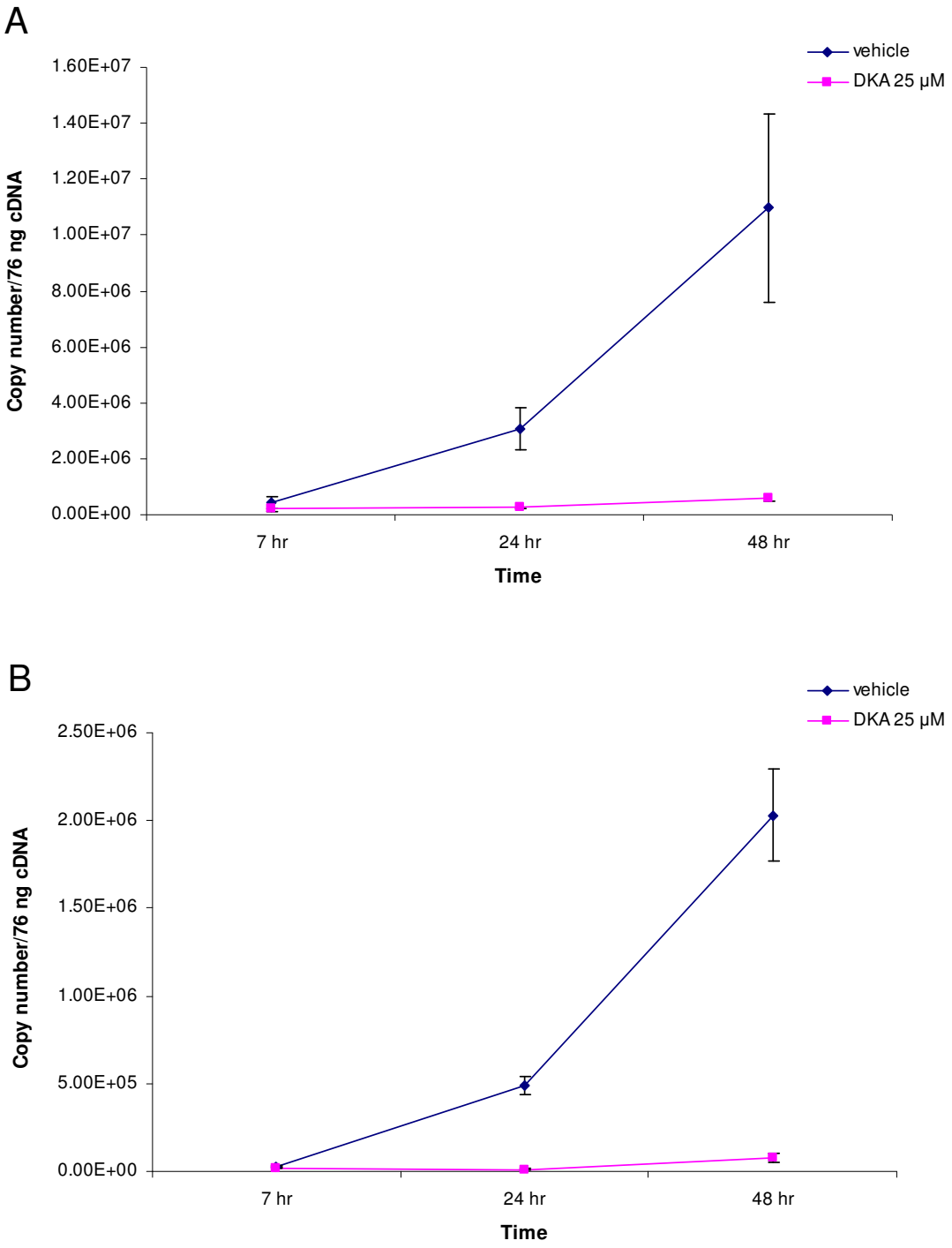

Figure 3-3. Integration is required for the propagation of VSVG pseudotyped HIV-1 NL4-3 env- RNA. Co-exposure to DKA greatly decreased the quantity of HIV-1 total RNA in both HBMECs (A) and U373 MAGI CXCR4 cells (B). Error bars represent standard error.

D. HBMECs synthesize a lower quantity of multiply spliced *rev* transcripts

Following integration of the HIV-1 cDNA into the host genome, transcription of early regulatory genes are induced by host factors and then subsequently much enhanced by the HIV-1 transactivating protein Tat. Transcripts encoding two major early regulatory proteins, Tat and Rev, are synthesized through the splicing of various exons. To assess the ability of HBMECs to mediate the synthesis of HIV-1 early transcripts, total RNA isolated from VSV-G pseudotyped HIV-1 NL4-3 env- exposed HBMECs and U373 MAGI CXCR4 cells were subjected to reverse transcription qRT-PCR detection and quantitation of *rev* transcripts. In both cell types, *rev* could be detected at 12 hr post-exposure. While *rev* accumulated and increased in U373 MAGI CXCR4 cells, the quantity of *rev* remained low and stable in HBMECs up to 96 hr (Figure 3-4). However, this diminished synthesis of *rev* transcripts in HBMECs does not seem to have a negative impact on HIV-1 whole genome or *gag* transcript amplification (Figure 3-1).

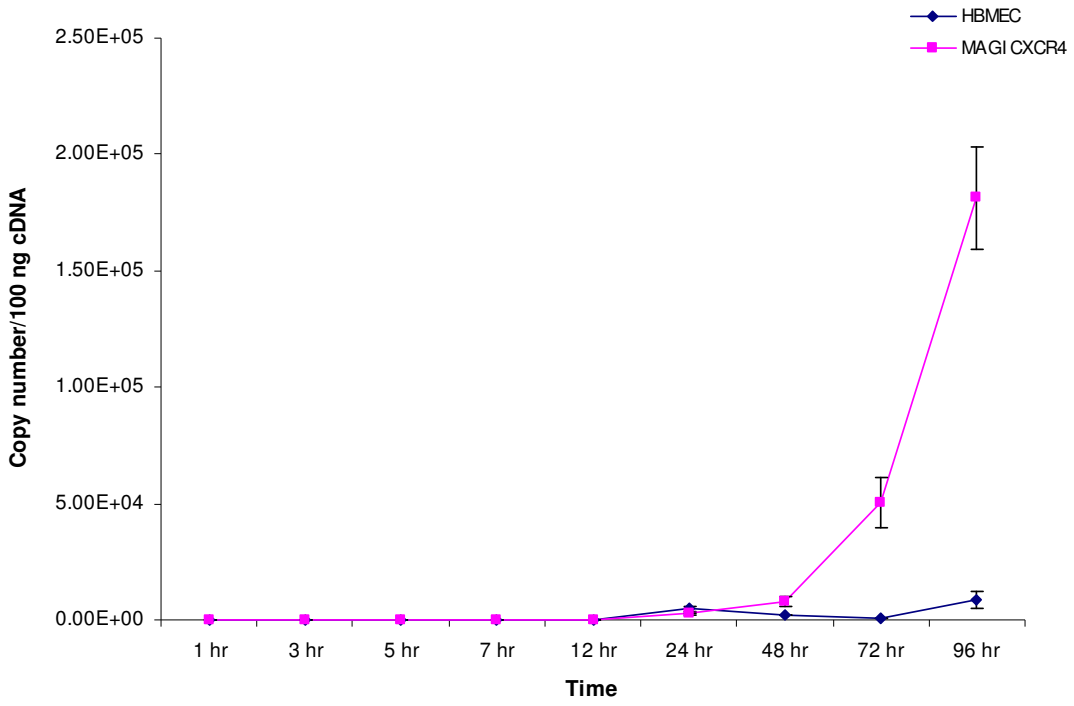

Figure 3-4. HBMECs synthesize a lower quantity of *rev* than MAGI cells. HBMECs and U373 MAGI CXCR4 cells were spinoculated with 0.2 MOI of VSV-G pseudotyped HIV-1 NL4-3 env- in parallel. Total RNA was isolated at various time post-exposure and subjected to reverse transcription qRT-PCR detection and quantitation of HIV-1 *rev*. Figure 3-4 is representative of two qRT-PCR runs of the same experiment. Error bars represent standard error.

E. HBMECs displayed alternative processing, and/or degradation, of HIV-1 Gag proteins

To assess the ability of HBMECs to synthesize viral structural proteins, cell lysates were collected from HBMECs and U373 MAGI CXCR4 cells exposed to VSV-G pseudotyped NL4-3 env-, then subjected to Western blot analysis for HIV-1 Gag proteins. The synthesis of Gag proteins involves the translation of two polyproteins, Pr55 Gag and Pr160 Gag-Pro-Pol, which are subsequently cleaved by HIV-1 protease to produce p17, the matrix protein (MA), p24, the nucleocapsid protein (CA), HIV-1 protease, HIV-1 integrase and HIV-1 reverse transcriptase. The polyclonal antibody (NIH Cat#4250) employed for this study reacts with both pre-processed polyproteins and Gag proteins going through various stages of cleavage and processing. As shown in Figure 3-5, in addition to the band representing p24 CA and in contrast to U373 MAGI CXCR4 cells, HBMECs yielded bands of various molecular weights below 24 kDa, the most prominent one being below 13 kDa. This result suggests that HBMECs are permissive of the translation and synthesis of p24. The identities of bands below 24 kDa in HBMEC lysate are unclear. Their cross-reactivity suggests that they could be of Gag protein origin, raising the possibility that HBMECs might be exerting alternative processing, and possibly degradation, on HIV-1 Gag. Kinetic-wise, in both cell types, there was a consistent presence of p24 throughout the early time points, except at

24 h, most likely the result of the degradation of p24 from internalized inoculums. However, in HBMECs, there was a diminished amount of p24 at 96 h, at which point the amount of molecular weight products below 13 kDa continued to accumulate.

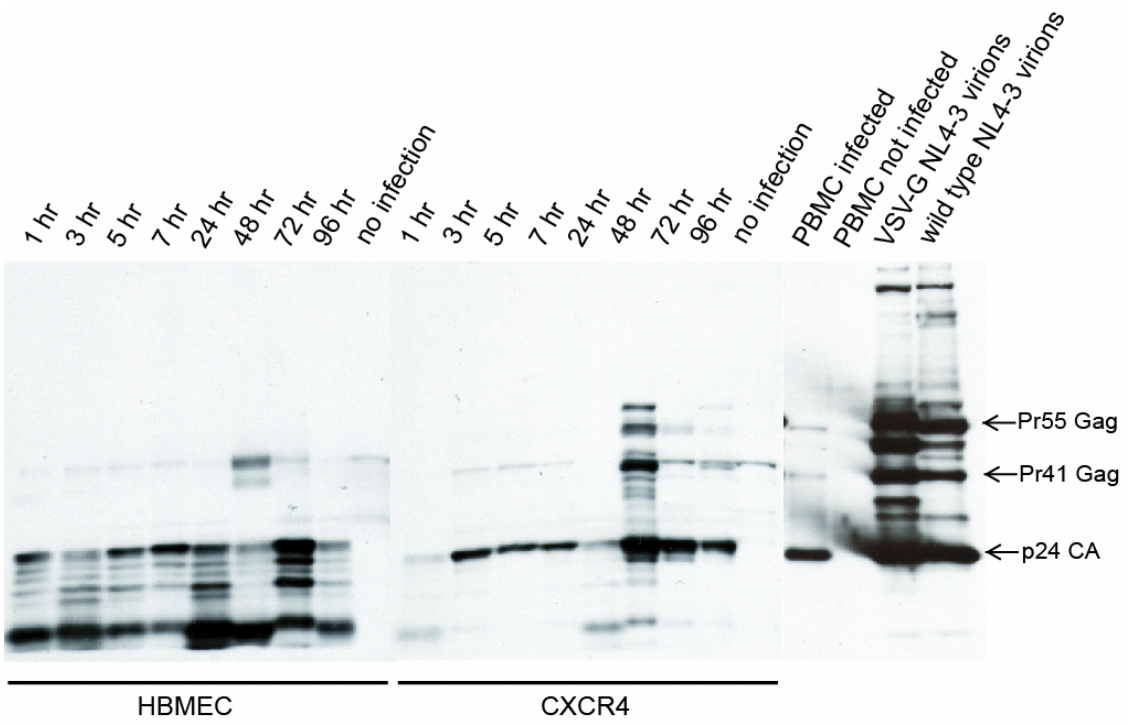

Figure 3-5. HBMECs are permissive of *gag* translation yet might exert alternative processing or degradation on Gag proteins. HBMECs and U373 MAGI CXCR4 cells were spinoculated with 0.2 MOI of VSV-G pseudotyped HIV-1 NL4-3 env- in parallel. Cell lysate was isolated at various time post-exposure and subjected to Western blot analysis for Gag. Figure 3-5 is representative of two Western blots from the same experiment.

F. HBMECs restrict the synthesis of transduced p24 capsid protein

To test the hypothesis that HBMECs might be specifically targeting p24 for degradation, HBMECs were exposed to a lentivirus, which encodes and confers ectopic p24 overexpression, and the fates of these capsid proteins were assessed in a time course using Western blot analysis. As shown in Figure 3-6, in contrast to U373 MAGI CXCR4 cells, HBMECs permitted the synthesis of p24 only up to 24 h. Thereafter, the amount of p24 decreased and the trend continued through the rest of the time course.

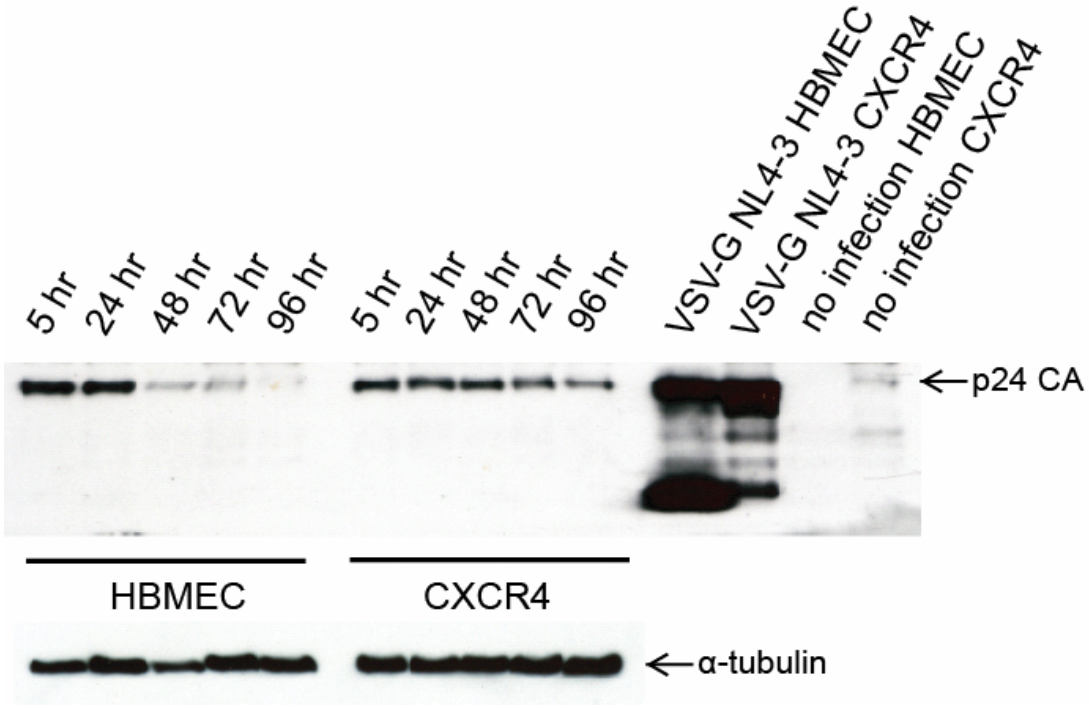

Figure 3-6. HBMECs restrict transduced p24 synthesis. HBMECs and U373 MAGI CXCR4 cells were transduced with a p24 encoding lentivector. p24 expression was assessed in a time course using Western blot analysis. Figure 3-6 is representative of two Western blots of the same experiment.

Discussion

HBMECs have been reported to be infected by HIV-1 in vivo but these findings have often been questioned on the grounds of technical limitations and difficulties in interpreting results. In vitro productive infection has been demonstrated but results were not reproducible. It is possible that the eventual outcome of HIV-1 infection of HBMECs depends considerably on viral and host factors, some of which have yet to be identified. The current study utilized a VSV-G pseudotyped HIV-1 NL4-3 virus which could bypass the receptor barrier to study the course of HIV-1 infection in HBMECs. Toward this aim, a series of qRT-PCR assays were developed which enabled sensitive and specific detection of HIV-1 nucleic acids that are indicative of various stages of the virus lifecycle. The findings here indicated that once internalized into the HBMEC cytoplasm, the HIV-1 genome is capable of reverse transcription, integration, and *gag* transcription and whole genome replication in HBMECs. However, compared to the glioblastoma indicator cell line which has been established to be permissive to HIV-1 infection, HBMECs permitted minimal *rev* transcription. In addition, HBMECs exhibit an unknown modification or processing, and possibly degradation, of HIV-1 p24 capsid protein.

For the current investigation, in vitro experiments were performed since they are more amenable to optimization and positive control measures. Indeed, the results presented here suggested that the methodologies

developed for this study offer several advantages over previous methods and addresses some of the technical challenges faced by previous studies. One of the biggest shortcomings with detection of HIV-1 antigen using immunohistochemistry on fixed tissues is the method's inability to distinguish between merely surface associated viruses and progeny viruses from a true infection event (Bissel *et al*., 2004). To prevent this same issue from detracting from the current in vitro study, pronase was employed in this study for cell dissociation and it was demonstrated that cell surface associated viruses can effectively be removed upon treatment (Figure 1-1). The second technical issue which often plagued in vitro virology studies is the suboptimal infectivity of wild type virus inoculum. This problem is often alleviated by using an increased input or reducing the volume in which the target cells are incubated. However, neither of these approaches was easily adaptable for the current study. Not only are the expansion of wild type HIV-1 primary isolate from PBMC co-culture and the production of VSV-G pseudotyped HIV-1 from 293T packaging cells labor intensive processes, but most of the time titers obtained are not very high. This problem could be solved by up-scaling production but this too would be expensive and time consuming. Reducing the volume of the inoculum also was not a viable solution. No data is available on the minimum volume that facilitates virus:cell contact without risking medium evaporation. With these issues in mind, the approach spinoculation method developed by O'Doherty was adopted. As shown in Figure 1-2,

compared to just two hours co-incubation, 1 hour co-incubation followed by 1 hour spinoculation resulted in an almost 20 fold increase in the *gag* genome detected. Analogous to minimizing the volume in which the cells are exposed to viruses, this method very possibly enhances HIV-1 infection by facilitating virus:cell contact. The data presented here also supports previous findings that HBMECs are capable of internalizing HIV-1 even in the absence of CD4 receptors (Liu *et al*., 2002).

A major criticism of previous studies employing in situ detection of PCR-amplified HIV nucleic acids on microdissected HBMECs from fixed tissues is the lack of quantitative information. Not only is the biological significance of detecting viral nucleic acids in a small sample of microdissected cells debatable, it is also not clear whether the detected signal originated from only one or a few attached virions or nucleic acids from a true infectious event. To address this issue, a series of qRT-PCR assays which specifically target viral nucleic acids representative of the various stages of the HIV-1 lifecycle were developed. Compared to previous techniques ELISA, immunohistochemistry, functional focal infectivity assay, and Southern blotting which is capable of only a limited extent of quantitation, qRT-PCR offers several advantages. First, this method allows the effective assessment of the extent and progress of HIV-1 infection by simply sampling and quantitating the different types of viral nucleic acids, since each is unique to a single key step

of the HIV-1 lifecycle. Second, qRT PCR is easy to optimize compared to other detection strategies since there are fewer intervening steps. Thus, not only there are relatively few parameters to be adjusted, but the ease with which they could be adjusted makes this methodology ideal for the adaptation to detecting different nucleic acid types. For the current study, once a primer set specific to the target nucleic acid was designed, the optimization for the annealing temperature was expedited by the Bio-Rad iQ5 iCycler thermocycler's capability of subjecting different rows of a 96-well plate to different annealing temperatures. In this way, a range of annealing temperatures was tested in one run and the annealing temperature that yielded the earliest threshold cycle (Ct) was used for any subsequent experiments. The third advantage of these PCR assays over other methodologies is that sensitive, specific, precise, and reproducible quantitation of target nucleic acids is relatively easy to achieve provided that the experiment parameters are optimized. As demonstrated in Figure 2-2, a linear range of 1×10^6- 1×10^1 was achieved with the detection and quantitation of late reverse transcribed (RT) product. Furthermore, the accuracy of this assay was demonstrated by the low standard deviations of the Ct values (intra-run 0.183-0.391, inter-run 0.04-0.753).

To study the course of HIV-1 infection in cell types that apparently do not express the required receptors, various methods have been devised to

bypass the entry requirement. For example, to study the course of HIV-1 infection in astrocytes, both transfection of a plasmid encoding the molecular clone of HIV-1 (Bencheikh *et al*., 1999) and cell lines transiently or stably transfected with HIV-1 DNA (Tornatore *et al*., 1994) have been employed. However, in addition to technical limitations inherent to these methods, one drawback common to both strategies is the inability to reproduce several key steps of the natural HIV-1 lifecycle. For example, not only is transfection inefficient for primary cells, but many of the essential steps of the HIV-1 life cycle, reverse transcription, pre-integration complex formation, nucleus entry, and integration into the host genome, are amiss when this method is employed. Toward the aim of achieving as closely as possible the natural course of an HIV-1 infection, a VSV-G pseudotyped NL4-3 *env* defective virus was employed for this study. Compared to wild type NL4-3 virus, VSV-G pseudotyped virus is capable of achieving a much more efficient infection, as shown in Figure 1-3. This has proven to be especially advantageous during the development and troubleshooting phase of the PCR assays. Coupled with the ability of U373 MAGI cells to get easily infected and visualized, the use of VSV-G virus not only to a large extent guaranteed infection but also provided a means for the evaluation and optimization of the PCR assays. In addition, since there are potentially unidentified host or viral determinants on cytoplasmic delivery of the HIV-1 genome, using the VSV-G pseudotyped

virus guaranteed cytoplasmic entry and permitted the examination for intracellular restriction downstream in HBMECs.

In the current study, using efficient infection, the possibility of HBMEC intracellular restriction to HIV-1 replication was explored. PCR viral kinetic studies here demonstrated that HBMECs permit a level of pseudotyped HIV-1 internalization comparable to the permissive U373 MAGI cell line. This is not surprising since the VSV-G receptor utilizes membrane phospholipids, which are present in all eukaryotic cells, for binding (Schlegel *et al*., 1983). Subsequent to binding and internalization via unspecific endocytosis, the VSV-G glycoprotein mediates membrane fusion triggered by the acidic pH in the late endosome or lysosome (Mastromarino *et al*., 1987), essentially delivering the viral genome into the cytoplasm. Since the *gag* transcript is a continuous mRNA unlike *rev*, which is synthesized from the splicing of two exons, a primer set which is specific to the *gag* mRNA or the HIV-1 whole genome wasn't able to be designed. For this reason, the result shown in Figure 3-1 is not indicative solely of *gag* mRNA, internalized whole genome from the inoculum, or newly synthesized whole genome. However, it is safe to assume that HIV-1 replication, indicated by the increase in *gag* signal detected over time arising from either *gag* messenger RNA or whole genome, did take place since reverse transcription was also shown to occur as indicated by the increase in late RT product (Figure 3-2). This interpretation is further

corroborated when *gag* detection was diminished with the administration of diketo acid (DKA), an integrase inhibitor (Figure 3-3). Overall, these results demonstrated that up to the point of integration into the host genome, HIV-1 is capable of a natural course of infection in HBMECs provided that the receptor requirement is bypassed.

The HIV-1 Rev protein is an early regulatory protein responsible for the nuclear export of singly spliced or unspliced mRNA which are instrumental for the translation and the final assembly of progeny virions. Given the important role that Rev serves in the viral lifecycle, it is no surprise that Rev can be the target of various cellular restrictive mechanisms. Previous studies on astrocytes, another CNS cell type which does not express CD4 but has been shown to permit infection by HIV-1 to various degrees, have shown that inefficient Rev function could be the cause of low levels of viral structural proteins in astrocytes (Neumann *et al*., 1995, Ludwig *et al*., 1999). In the current study, HBMECs exhibited a much diminished synthesis of *rev* transcripts in contrast to U373 MAGI cells, suggesting the possibility of an unknown cellular factor or a novel mechanism restricting the progression of HIV-1 lifecycle. Further experiments should be pursued to assess the level of Rev protein expression to determine if this diminished amount of mRNA has an impact on the translation of Rev protein. In other words, is the level of Rev protein determined by the absolute amount of *rev* transcripts or by the stability

of *rev* transcripts in HBMECs? At the first glance, it would seem that the latter is the case since as shown in Figure 3-1, the level of *gag* was not affected despite the diminished level of *rev*. However, it should be noted that Rev protein is responsible for shuttling singly spliced structural protein mRNA, including *gag*, or unspliced whole genome RNA out of the nucleus but has no influence over the *synthesis* of these scripts. Further experiments are needed to demonstrate the localization of singly and unspliced mRNAs to further shed light on the nature and functional consequence of this diminished level of *rev* mRNA. Furthermore, for future studies, it would be interesting to assess if this observation also extends to other multiply spliced mRNAs, such as *tat*.

In addition to possible cellular restriction at the level of viral mRNA synthesis, the current study also showed that HBMECs might be harboring a modification, and possibly degradation, of the HIV-1 p24 capsid protein (Figure 3-5). At this stage, the cellular factor involved, mechanism and functional consequence of this observation are not yet clear. Determining the identity of the bands below 24 kDa size would be a crucial step to addressing the aforementioned concerns. To test the hypothesis that p24 capsid protein is being targeted specifically for modification or degradation, a lentiviral vector overexpressing p24 alone was transduced into HBMECs (Figure 3-6). In comparison to when the whole genome is expressed, the gradual decrease in the amount of p24 is more pronounced. However, in contrast, the bands

below 24 kDa molecular weight were not observed. One possible explanation for this difference might be that when the whole viral genome is expressed, there is a viral factor, unidentified or part of the Gag polypeptide precursor, that associates with the p24 capsid and makes the degradation products evident by Western blotting. For future studies, to investigate if this possible degradation mechanism could have a functional consequence on virus titer released from HBMECs, a VSV-G pseudotyped fully functional HIV-1 can be used. Then the level of p24 in the supernatant can be monitored and compared to U373 MAGI cells subjected to the same treatment.

In summary, the current study demonstrated that HBMECs are permissive to HIV-1 infection yet might harbor multiple intracellular blocks to important events in the viral lifecycle. Further experiments are needed to identify the viral and host factors which determine the eventual outcome of an infection event, the molecular mechanism(s) behind these modulations, and how they might be exploited for the discovery and development of novel therapeutic measures.

References

Alvarez LS, Munoz-Fernandez MA (2002) A new possible mechanism of human immunodeficiency virus type 1 infection of neural cells. *Neurobiol. Dis.* **11**: 469-478

An SF, Groves M, Giometto B, Beckett AA, Scaravilli F (1999) Detection and localization of HIV-1 DNA and RNA in fixed adult AIDS brain by polymerase chain reaction/in situ hybridization technique. *Acta. Neuropathol.* **98**: 481-487

Anderson CE, Pauly B, Brannan FW, Chiswick A, Brack-Werner R, Simmonds P, Bell JE (2003) Relationship of Nef-positive and GFAP-reactive astrocytes to drug use in early and late HIV infection. *Neuropathology and Applied Neurobiology* **29**: 378-388

Andras IE, Pu H, Deli MA, Nath A, Hennig B, Toborek M (2003) HIV-1 Tat protein alters tight junction protein expression and distribution in cultured brain endothelial cells. *J. Neurosci Res.* **15**: 255-65

Andrew V, Albright JS, Harouse JM, Lavi E, O'Connor M, Gonzales-Scarano F (1996) HIV-1 infection of cultured human adult oligodendrocytes. *Virology* **217**: 211-219

Argyris EG, Archeampong E, Nunnari G, Mukhtar M, Williams KJ, Pomerantz RJ (2003) Human immunodeficiency virus type 1 enters primary human brian microvascular endothelial cells by a mechanism involving cell surface proteoglycans independent of lipid rafts. *J. Virol.* **77**: 12140-12151

Aylward EH, Brettschneider PD, McArthur JC, Harris GJ, Schlaepfer TE, Henderer JD, Barta PE, Tien AY, Pealson GD (1995) Magnetic resonance imaging measurement of gray matter volume reductions in HIV dementia. *Am. J. Psychiatry.* **152**: 987-994

Banks WA, Freed EO, Wolf KM, Robinson SM, Franko M, Kumar VB (2001) Transport of human immunodeficiency virus type 1 pseudoviruses across the blood-brain barrier: role of envelope proteins and absorptive endocytosis. *J. Virol.* **75**: 4681-4691

Bencheikh M, Bentsman g, Sarkissian N, Canki M, Volsky DJ (1999) Replication of different clones of human immunodeficiency virus type 1 in primary fetal human astrocytes: enhancement of viral gene expression by Nef. *J. Neuroviol.* **5**: 115-124

Berger JR, Arendt G (2000) HIV dementia: the role of the basal ganglia and dopaminergic systems. *J. Psychopharmacol.* **14**: 214-221

Bissel SJ, Wiley CA (2004) Human immunodeficiency virus infection of the brain: pitfalls in evaluating infected/affected cell populations. *Brain Pathol.* **14**: 97-108

Butler SL, Hansen MST, Bushman FD (2001) A quantitative assay for HIV DNA integration in vivo. *Nature Medicine* **7**: 631-634

Canki M, Thai JN, Chao W, Ghorpade A, Potash MJ, Volsky DJ (2001) Highly productive infection with pseudotyped human immunodeficiency virus type 1 (HIV-1) indicates no intracellular restrictions to HIV-1 replication in primary human astrocytes. *J. Virol.* **75**: 7925-7933

Carroll-Anzinger D, Vyacheslav Adarichev AK, Kashanchi F, Al-Harthi L (2007) Human immunodeficiency virus-restricted replication in astrocytes and the ability of gamma interferon to modulate this restriction are regulated by a downstream effector of the Wnt signaling pathway. *J. Virol.* **81**: 5864-5871

Chaudhuri A, Duan F, Morsey B, Persidsky Y, Kanmogne GD (2007) HIV-1 activates proinflammatory and interferon-inducible genes in human brain microvascular endothelial cells: putative mechanisms of blood-brain barrier dysfunction. *J. Cereb. Blood Flow Metab.* [Epub ahead of print]

Cheng-Mayer C, Rutka JT, Rosenblum ML, McHugh T, Stites DP, Levy JA (1987) Human immunodeficiency virus can productively infect cultured human glial cells. *Proc. Natl. Acad. Sci. U. S. A.* **84**: 3526-3530

Ellis R, Langford D, Masliah E (2007) HIV and antiretroviral therapy in the brain: neuronal injury and repair. *Nat. Rev. Neurosci.* **8**: 33-44

Fischer-Smith TRJ (2005) Evolving paradigms in the pathogenesis of HIV-1 associated dementia. *Expert Rev. Mol. Med.* **7**: 1-26

Foos TM, Wu JY (2002) The role of taurine in the central nervous system and the modulation of intracellular calcium homeostasis. *Neurochem. Res.* **27**: 21-26

Gonzalez-Scarano F, Martin-Garcia J (2005) The neuropathogenesis of AIDS. *Nat. Rev. Immunol.* **5**: 69-81

Gyorkey FMJ, Gyorkey P (1987) Human immunodeficiency virus in brain biopsies of patients with AIDS and progressive encephalopathy. *Journal of Infectious Disease* **155**: 870-876

Hao HN, Lyman WD (1999) HIV infection of fetal human astrocytes: the potential role of a receptor-mediated endocytic pathway. *Brain Res.* **823**: 24-32

Harouse JM, Kunsch C, hartle HT, Laughlin MA, Hoxie JA, Wigdahl B, Gonzalez-Scarano F (1989) CD4-independent infection of human neural cells by human immunodeficiency virus type 1. *J. Virol.* **63**: 2527-2533

Hinkin CH, van Gorp WG, Mandelkern MA, Gee M, Satz P, Holston S, marcotte TD, Evans G, Paz DH, Ropchan JR (1995) Cerebral metabolic change in patients with AIDS: report of a six-month follow-up using positron-emission tomography. *J. Neuropsychiatry. Clin. Neurosci.* **7**: 180-187

Kanmogne GD, Grammas P, Kennedy RC (2000) Analysis of human endothelial cells and cortical neurons for susceptibility to HIV-1 infection and co-receptor expression. *J. Neurovirol.* **6**: 519-528

Kelly J, Beddall MH, Yu D, Iyer SR, Marsh JW, Wu Y (2008) Human macrophages support persistent transcription from unintegrated HIV-1 DNA. *Virology*. **15**: 300-312

Langford TD, Letendre SL, Marcotte TD, Ellis RJ, McCutchan JA, Grant I, Mallory ME, Hansen LA, Archibald S, Jernigan T, Masliah E; HNRC Group (2002) Severe, demyelinating leukoencepahlopathy in AIDS patients on antiretroviral therapy. *AIDS.* **3**: 1019-1029

Li J, Bentsman G, Potash MJ, Volsky DJ (2007) Human immunodeficiency virus type 1 efficiently binds to human fetal astrocytes and induces neuroinflammatory responses independent of infection. *BMC Neurosci.* **8**: 31

Liu NQ, Lossinsky AS, Popik W, Li X, Gujuluva C, Kriederman B, Roberts J, Pushkarsky T, Bukrinsky M, Witte M, Weinand M, Fiala M (2002) Human immunodeficiency virus type 1 enters brain microvascular endothelia by macropinocytosis dependent on lipid rafts and the mitogen-activated protein kinase signaling pathway. *J. Virol.* **76**: 6689-6700

Liu Y, Liu H, Kim BO, Gattone VH, Li J, Nath A, Blum JM, He JJ (2004) CD-4 independent infection of astrocytes by human immunodeficiency virus type 1: requirement for the human mannose receptor. *J. Virol.* **8**; 4120-4133

Lugwig E, Ceccherini-Silberstein F, van Empel J, Erfle V, Neumann M, Brack-werner R (1999) Diminished Rev-mediated stimulation of human immunodeficiency virus type 1 is a hallmark of human astrocytes. *J. Virol.* **73**: 8279-8289

Mankowski JL, Spelman JP, Ressetar HG, strandberg JD, laterra J, Carter DL, Clements JE, Zink MC (1994) Neurovirulent simian immunodeficiency virus replicates productively in endothelial cells of the central nervous system in vivo and in vitro. *J. Virol.* **68**: 8202-8208

Mariani R, Rutter G, Harris ME, Hope TJ, Krausslich HG, Landau NR (2000) A block to human immunodeficiency virus type 1 assembly in murine cells. *J. Virol.* **74**: 3859-3870

Mastromarino P, Conti C, Goldoni P, Hauttecoeur B, Orsi N (1987) Characterization of membrane components of the erythrocyte involved in vesicular stomatitis virus attachment and fusion at acidic pH. *J. Gen. Virol.* **68**: 2359-2369

Meucci O, Fatatis A, Simen AA, Bushell TJ, Gray PW, Miller RJ (1998) Chemokines regulate hippocampal neural signaling and gp120 neurotoxicity. *Proc. Natl. Acad. Sci. U. S. A.* **24**: 14500-14505

Moses AV, Strenglein SG, Strussenberg JG, Wehrly K, chesebro B, Nelson JA (1996) Sequences regulating tropism of human immunodeficiency virus type 1 for brain capillary endothelial cells map to a unique region on the viral genome. *J. Virol.* **6**: 3401-3406

Neumann M, Felber BK, Kleinschmidt A, Froese B, Erfle V, Pavlakis GN, Brack-Werner R (1995) Restriction of human immunodeficiency virus type 1 production in a human astrocytoma cell line is associated with a cellular block in Rev function. *J. Virol.* **69**: 2159-2167

Newton TF, Leuchter AF, Walter DO, Van Gorp WC, Stern CE, Mandelkern M, Weiner H (1993) EEG coherence in men with AIDS: association with subcortical metabolic activity. *J. Neuropsychiatry Clin. Neurosci.* **5**: 316-321

Nuovo GJ, Gallery F, MacConnell P, Braun A (1994) In situ detection of polymerase chain reaction-amplified HIV-1 nucleic acids and tumor necrosis factor-alpha RNA in the central nervous system. *Am. J. Pathol.* **144**: 659-666

O'Doherty U, Swiggard WJ, Malim MH (2000) Human immunodeficiency virus type 1 spinoculation enhances infection through virus binding. *J. Virol.* **74**: 10074-80

Patel CA, Mukhtar M, Harley S, Kulkosky J, Pomerantz RJ (2002) Lentiviral expression of hIV-1 Vpr induces apoptosis in human neurons. *J. Neuroviol.* **8**: 86-99

Poland SD, Rice GP, Dekaban GA (1995) HIV-1 infection of human brain-derived microvascular endothelial cells in vitro. *J. Acquir. Immune Defic. Syndr. Hum. Retrovirol.* **15**: 437-445

Rottenberg DA, Moeller JR, Strother SC, Sidtis JJ, Navia BA, Dhawan V, Ginos JZ, Price RW (1987) The metabolic pathology of the AIDS dementia complex. *Ann. Neurol.* **22**: 700-706

Sakuma R, Noser JA, Ohmine S, Ikeda Y (2007) Rhesus monkey TRIM5α restricts HIV-1 production through rapid degradation of viral Gag polyproteins. *Nature Medicine* **13**: 631-635

Schwartz S. Felber BK, Benko DM, Fenyo EM, Pavlakis GN (1990) Cloning and functional analysis of multiply spliced mRNA species of human immunodeficiency virus type 1. *J. Virol.* **64**; 2519-2529

Schlegel R, Tralka TS, Willingham MC, Pastan I (1983) Inhibition of VSVG binding and infectivity by phosphatidylserine: is phosphatidylserine a VSV-binding site? *Cell* **32**: 639-646

Song L, Nath A, Geiger JD, Moore A, Hochman S (2003) Human immunodeficiency virus type 1 Tat protein directly activates neuronal N-methyl-D-aspartate receptors at an allosteric zinc-sensitive site. *J. Neurovirol.* **9**: 399-403

Takahashi K, Wesselingh SL, Griffin DE, McArthur JC, Johnson RT, Glass JD (1996) Localization of HIV-1 in human brain using polymerase chain reaction/in situ hybridization and immunocytochemistry. *Ann. Neurol.* **39**: 705-711

Tornatore DK, Meyers K, Atwood W, Conant K, Major EO (1994) Temporal patterns of human immunodeficiency virus type 1 transcripts in human fetal astrocytes. *J. Virol.* **68**: 93-102

Vandegraaff N, Kumar R, Hocking H, Burke TR, Mills J, Rhodes D, Burrel CJ, Li P (2001) Specific inhibition of human immunodeficiency virus type 1 (HIV-1) integration in cell culture: putative inhibitors of HIV-1 integrase. *Antimicrobial Agents and Chemotherapy* **45**: 2510-2516

Wang T, Rumbaugh JA, Nath A (2006) Viruses and the brain: from inflammation to dementia. *Clin. Sci.* **110**: 393-407

Ward JM, O'Leary TJ, Baskin GB, Benveniste R, Harris CA, Nara PL, Rhodes RH (1987) Immunohistochemical localization of human and simian immunodeficiency viral antigens in fixed tissue sections. *Am. J. Pathol.* **127**: 199-205

Wiley CA, Schrier RD, Nelson JA, Lampert PW, Oldstone MB (1986) Cellular localization of human immunodeficiency virus infection within the brains of acquired immune deficiency syndrome patients. *Proc. Natl. Acad. Sci. U. S. A.* **83**: 7089-7093